Fracture Analysis of Non-coplanar Crack Extension Under Mixed-mode Loading by the Crack Closure Integral Method

F. -G. BUCHHOLZ and H. A. RICHARD
Institute of Mechanics, University of Paderborn, Pohlweg 47-49, D-4790, Paderborn, FRG

ABSTRACT

The crack closure integral method (CCI-meth.) has proved to be a numerically highly effective procedure for the fracture analysis of various crack problems in plane elasticity. In this paper it is shown that the CCI-method can also be utilized for the fracture analysis of non-coplanar crack extension in a compact tension shear specimen (CTS-spec.) under mixed-mode loading. The investigation is focusing on the directions the new crack is taking when kinking off from the original crack plane and when further crack extension is taking place. The results obtained straight forwardly by the CCI-method or by other mixed-mode fracture criteria are being compared with crack paths obtained experimentally by mixed-mode fracture of CTS-specimens. Hereby the tendency of the kinked crack is confirmed to extend preferably in that direction, which will create predominant mode-I conditions at the actual crack tip.

KEYWORDS

Crack closure integral method; mixed-mode fracture criteria; direction of kinking cracks; non-coplanar crack extension.

INTRODUCTION

Mixed-Mode fracture is an important subject in fracture mechanics due to the fact, that mixed-mode crack tip conditions do occure in engineering practice under various geometrical-, loading- and material conditions (Gdoutos, 1984; Richard, 1984). For mixed-mode fracture two main problems have to be solved. The first problem also arising in pure mode-I fracture is the question on the beginning of mixed-mode fracture with respect to the fracture toughness of the material. The second and new problem with mixed-mode fracture is the question on the direction or angle the crack will take when kinking off from its original plane under mixed-mode crack tip conditions. Both questions may be answered by the various mixed-mode fracture criteria that have been proposed, but interesting enough rather scattering or even contradictionary predictions are given (Richard, 1984; Erdogan and Sih, 1963; Hussain et al., 1974; Nuismer, 1975; Amestoy et al., 1980).

In this paper the straight forward and numerically highly effectiv crack closure integral method (Rybicki and Kanninen, 1977; Buchholz and Kanninen, 1986) is utilized for the fracture analysis of mixed-mode fracture created in CTS-specimens. Hereby emphasis it put on the question which direction or crack angle the kinking crack will take and the further directions it will follow with further extension. For this investigation the main advantage of the CCI-method is the fact, that it delivers simultaneously the separated engergy release rate $G_i(a)$, i = I,II for the origanally plane crack and moreover straight forwardly in the same way $G_i(a+\Delta\bar{a},\phi)$ for the kinked crack, having the additional finite crack extension $\Delta\bar{a}$ in a direction forming the crack angle ϕ relative to the original crack plane. The same procedure applies for any further finite crack extension $n\Delta a$ possibly altering its direction again relative to that one of the preceeding crack extension $(n-1)\Delta\bar{a}$.

The obtained results will be discussed with respect to the experimental results and to the predictions given by the hypotheses of maximum energy release rates (Hussain et al., 1974, Nuismer, 1975; Amestoy et al., 1980) or maximum tangential stress (Erdogan and Sih, 1963) and of subsequent results like vanishing mode-II conditions for the extended crack tip.

CRACK CLOSURE INTEGRAL METHOD (CCI-METHOD)

Referring to Fig. 4 and its notations for a pure Mode I condition IRWIN's well known crack closure integral relation is give by

$$G_I(a) = \lim_{\delta a \to 0} \frac{2}{\delta a} \int_{x=0}^{x=\delta a} \frac{1}{2}\, \sigma_{yy}(r=x,\phi=0,a)\; u_y(r=\delta a-x,\phi=\pi,a+\delta a)\,dx \qquad (1)$$

Equation (1) delivers the energy release rate $G_I(a)$ on the basis of the work to be done in order to close the crack of lenght a+δa by an amount δa. According to Buchholz and Kanninen (1986) Eq. (1) can be transformed into the following FE-representation (CCI-method)

$$G_I(a+\Delta a/2) = \frac{1}{t}\,\frac{1}{2\Delta a}\left(F_{y,i}(a)\,\Delta u_{y,i-2}(a+\Delta a) + F_{y,i+1}(a)\,\Delta u_{y,i-1}(a+\Delta a)\right) \qquad (2)$$

holding for the LSE-discretisation as given in Fig. 5. In Eq. (2) $F_{y,j}(a)$ and $\Delta u_{y,j}(a+\Delta a)$ are denoting corresponding nodal point forces and relative nodal point displacements, respectively and t is standing for the specimen's thickness. It is emphasized that Eq. (2) is not only holding for finite crack extensions $\Delta a \gg 0$ but is numerically exact for the actual LSE-discretisation under consideration. As crack opening and crack closure are reversible processes in any elastic configuration this statement also is holding for a finite crack extension $\Delta\bar{a}$ forming a crack angle ϕ relative to the original crack plane or to the direction of the preceeding crack extension. Hence in a local crack tip coordinate system of the kinked crack the energy release rates are given as follows according to the CCI-method

$$G_I(a+\Delta\bar{a}/2,\phi) = \frac{1}{t}\,\frac{1}{2\Delta\bar{a}}\left(F_{y,i}(a,\phi)\,\Delta u_{y,i-2}(a+\Delta\bar{a},\phi) + F_{y,i+1}(a,\phi)\,\Delta u_{y,i-1}(a+\Delta\bar{a},\phi)\right) \qquad (3)$$

$$G_{II}(a+\Delta\bar{a}/2,\phi) = \frac{1}{t}\,\frac{1}{2\Delta\bar{a}}\left(F_{x,i}(a,\phi)\,\Delta u_{x,i-2}(a+\Delta\bar{a},\phi) + F_{x,i+1}(a,\phi)\,\Delta u_{x,i-1}(a+\Delta\bar{a},\phi)\right) \qquad (4)$$

FRACTURE ANALYSIS OF NON-COPLANAR CRACK EXTENSION

In Fig. 1 the assembled CTS-specimen (Fig. 2) and the loading device is to be seen mounted together in a tensile testing machine. By the aid of the special loading device the applied load F is acting under an angle α relative to the cross section AB of the specimen, containing the straight edge crack of lenght a. Hereby various loading conditions can be created reaching from pure mode I (α = 0 deg.) via mixed-mode (0 < α < 90) to pure mode II conditions (α = 90 deg.). The correlated quantitative values $K_i(a)$, i = I,II (K1-2CF, K2-2CF graphs) calculated on the basis of the LSE-discretisation of Fig. 6 and Eqs. (3) and (4) with $\phi = 0$ and $\Delta\bar{a} = \Delta a$ are plotted in Fig. 7 (Buchholz et al., 1987). They are in excellent agreement with the K1- and K2-SEF graphs in Fig. 7, representing a reference solution based on a hybrid singular crack tip element directly delivering the stress intensity factors in question (Schnack and Wolf, 1978).

The design of the CTS-specimen and of the special loading device has been proposed by Richard (1981) on the basis of extensive photoelastic and FE-investigations. A set of CTS-specimens fractured under mixed-mode loadings varying from α = 0 deg. (Mode I) with steps of Δα = 15 deg. to α = 90 deg. (Mode II) are given in Fig. 3. Distinctly the effects of the increasing load angle α on the kink angle φ of the extending crack and on the following instable crack growth are to be seen. The experimentally obtained crack paths (Fig. 3) have been digitized and incorporated into the FE-model of the CTS-specimen as illustrated in Fig. 8.

Now we will focus our interest to one typical mixed-mode crack path, obtained experimentally for α = 60 deg. The mixed-mode conditions at the crack tip are characterised by the stress intensity factors $K_i(a_o,\alpha)$, i = I,II, which can readily be determined from the correlated $G_i(a_o,\alpha)$-values, calculated by the aid of the CCI-method for the original coplanar crack a_o. In case of crack extension under this distinctly mixed-mode situation (for quantitative values see Fig. 7, α = 60 deg.) the crack will kink out of its original plane. According to the maximum tangential stress criterion ($\sigma_{\phi max}$-crit., Erdogan and Sih, 1963) the direction is given by

$$\frac{\partial}{\partial\phi}\left(\sigma_\phi(\phi,r)\right)_{\phi=\phi_o} = 0 \quad \text{and} \quad \frac{\partial^2}{\partial\phi^2}\left(\sigma_\phi(\phi,r)\right)_{\phi=\phi_o} < 0 \quad \text{with} \qquad (5)$$

$$\sigma_\phi(\phi,r) = \frac{1}{\sqrt{2\pi r}}\,\cos\frac{\phi}{2}\left(K_I\cos^2\frac{\phi}{2} - \frac{3}{2}\,K_{II}\sin\phi\right) \qquad (6)$$

denoting the tangential stress in a crack tip polar coordinate system. For r = const. = 0.05 a_o the variation of σ_ϕ with φ is plotted in Fig. 9 predicting a kink angle of $\phi_{o,\,TANS}$ = 43,9 deg. which is nearly coinciding with the experimentally observed crack angle $\phi_{o,EXP}$ = 44,5 deg.. Before we analyse the same situation by the aid of the CCI-method it should be emphasized that the $\sigma_{\phi max}$-criterion is entirely based on the crack tip stress field of the original coplanar crack of lenght a_o.

In contrast to that we have to consider an additional finite crack extension $\Delta\bar{a}$ with varying crack angles $\phi \neq (a_o, \Delta\bar{a})$ in order to utilize the CCI-method for this investigation. The results obtained for $\Delta\bar{a} = 0.05\ a_o$ and $\phi = \phi_{o,EXP} \pm \Delta\varepsilon_i$, i = 1,2 are plotted in Fig. 10 giving evidence that the direction $\phi_{o,GMAX}$ = 42,5 deg. (GG-60 graph) of maximum energy release rate for the finite crack extension $\Delta\bar{a}$ is very near to the experimentally observed crack angle of $\phi_{o,EXP}$ = 44,3 deg.. Moreover the plots of the separated energy release rates $G_i(\Delta\bar{a},\phi)$, i = I,II (G1-, G2-60 graphs) are indicating that

the directions of $G(\Delta\bar{a},\phi) \rightarrow$ max. and $G_{II}(\Delta\bar{a},\phi) \rightarrow$ min. are coinciding. This is in agreement with conclusions from the $\sigma_{\phi max}$ - crit. and other energy release rate criteria (Nuismer, 1975; Amestoy et al., 1980). The numerical results for α = 30 and 90 deg. (pure mode II loading) are leading to the same conclusions (Steller, 1988).

As discussed before, the CCI-method can straight forwardly be used for the analysis of further finite crack extensions $\Delta\bar{a}$, following the experimentally obtained crack path (α = 60 deg.). See Fig. 11 for $\Delta a = 2\Delta\bar{a}$ and Fig. 12 for $\Delta a = 3\Delta\bar{a}$. For these crack extensions a remarkable and increasing difference is to be seen between the experimental results and the direction locally leading to $G(\Delta\bar{a},\phi) \rightarrow$ max. or $G_{II}(\Delta\bar{a},\phi) \rightarrow$ min.. This is not surprising because the crack path modelled in the FE-analysis was taken from load controlled experiments, in which the CTS-specimen was fractured unstable and completely after crack kinking occured. This means the unstable running crack can not follow instantaneously the rapidly changing stress fields. But first results from running displacement controlled tests shown that under further quasistatic conditions the crack show further tendencies to follow G_{max}- or G_{IImin}-directions. That this tendency is inherent in unstable crack growth too is indicated by the results presented in Figs. 13 and 14. Here the two crack tip positions before and after the second kink (shortly before complete separation of the fractured CTS-specimen (Fig. 8) have been analysed by the aid of the CCI-method. Before that kink, the unstable crack is far away from following the quasistatic G_{max}-direction (Fig. 13) but, interesting enough, after kinking it is near by (Fig. 14). This is an interesting result, although it is clear that the experimental boundary conditions at that stage of the experiment may differ strongly from those holding for the corresponding quasistatic FE-analysis.

CONCLUSIONS

This investigation has shown that the CCI-method can straight forwardly be utilized for the analysis of cracks extending and kinking under highly mixed-mode conditions. For this complicated type of problem the property of delivering simultaneously the separated energy release rates is of great advantage.

REFERENCES

Amestoy, M. et al. (1980). In: Advances in Fracture Research (D. Francois, Ed.), Pergamon Press, Oxford, 107-113.

Buchholz, F.-G. and M.F. Kanninen (1986). Paper pres. at 1. World Congr. on Comput. Mech. (WCCM 1), Austin, Texas.

Buchholz, F.-G. et al. (1987). In: Numerical Methods in Fracture Mechanics (A.R. Luxmoore et al., Eds.), Pineridge Press, Swansea, 641-656.

Erdogan, F., G.C. Sih (1963). J. of Basic Engng., 85, 519-525.

Gdoutos, E.E.(1984). Problems of Mixed Mode Crack Propagation, Martinus Nijhoff Publ., The Hague.

Hussain, R.J. et al. (1974). ASTM STP 560, 2-28.

Nuismer, R.J. (1975). Int. J. of Fracture, 11, 245-250

Richard, H.A. (1981). Int. J. of Fracture, 17, R 105-R 107.

Richard, H.A. (1984). In: Advances in Fracture Research (S.R. Valluri et al., Eds.), Pergamon Press, Oxford, 3337-3344.

Rybicki, E.F., M.F. Kanninen (1977). Engng. Fracture Mech., 9, 931-938.

Schnack, E., M. Wolf (1978). Int. J. Num. Meth. Engng., 12 963-975.

Steller, G. (1988), Project Work, Inst. of Mechanics,Univ. of Paderborn

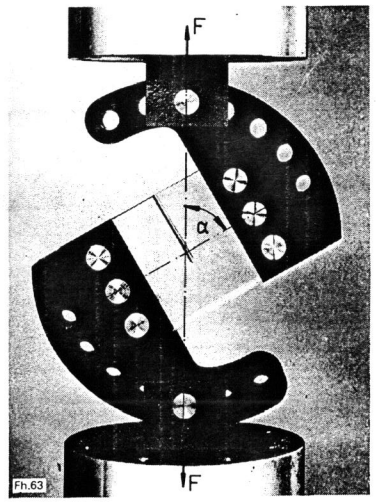

Fig. 1 Loading device with CTS-specimen (mixed-mode loading, α = 60 deg.)

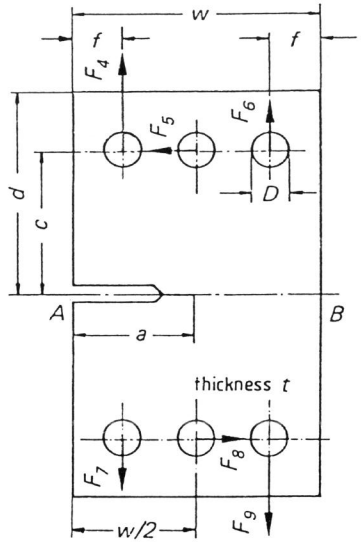

Fig. 2 Dimensions of the CTS-specimen (w = 80 mm, thickness t = 10-30 mm)

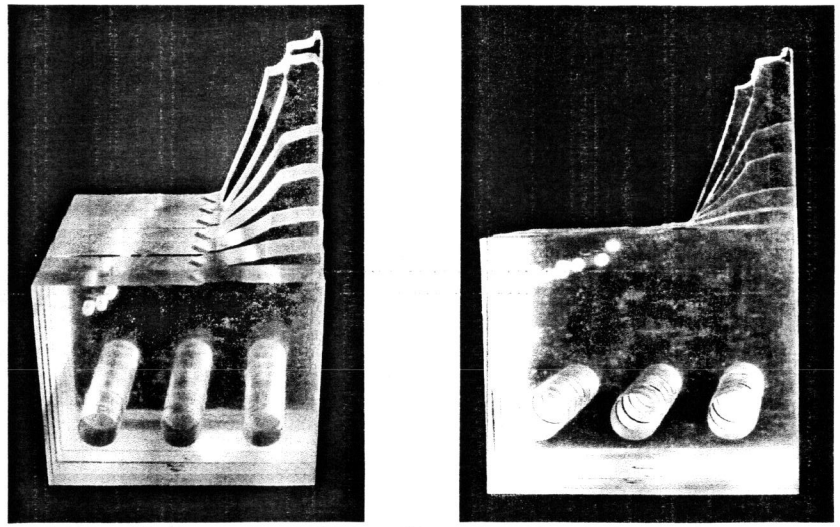

Fig. 3 CTS-specimens from PMMA fractured under mixed-mode loadings (α = 0-90 deg. with $\Delta\alpha$ = 15 deg.)

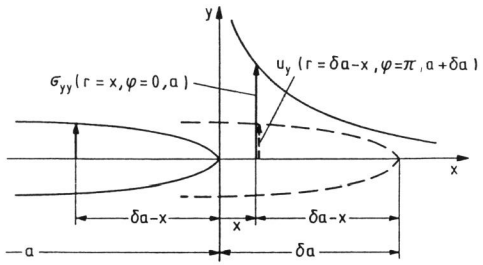

Fig. 4 Analytical crack closure integral method (lim $\delta a \to 0$)

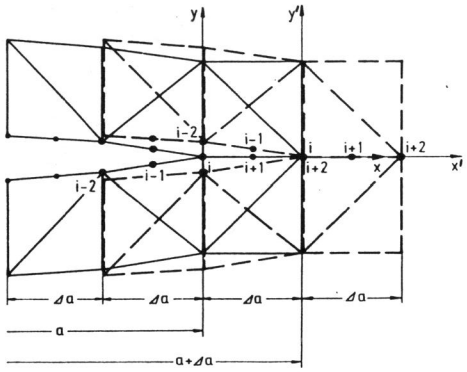

Fig. 5 Numerical crack closure integral method ($\Delta a >> 0$)

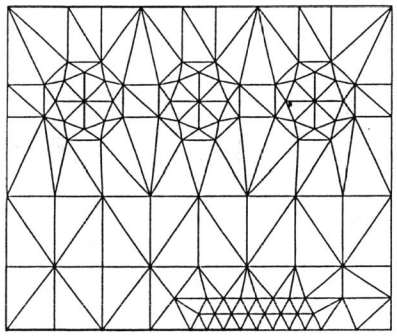

Fig. 6 FE-discretisation of the CTS-specimen with crack lenght a_0

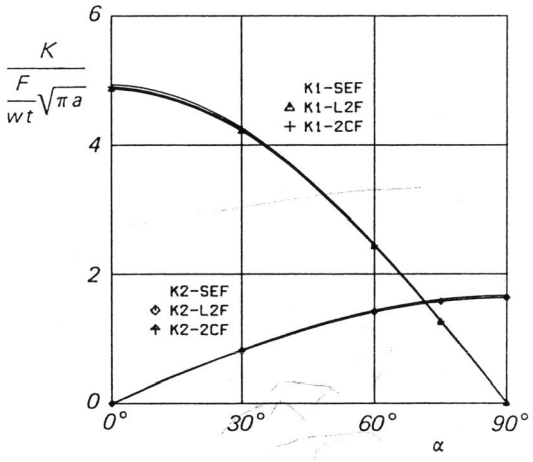

Fig. 7 Variation of stress intensity factors for the CTS-specimen with angle α of applied load

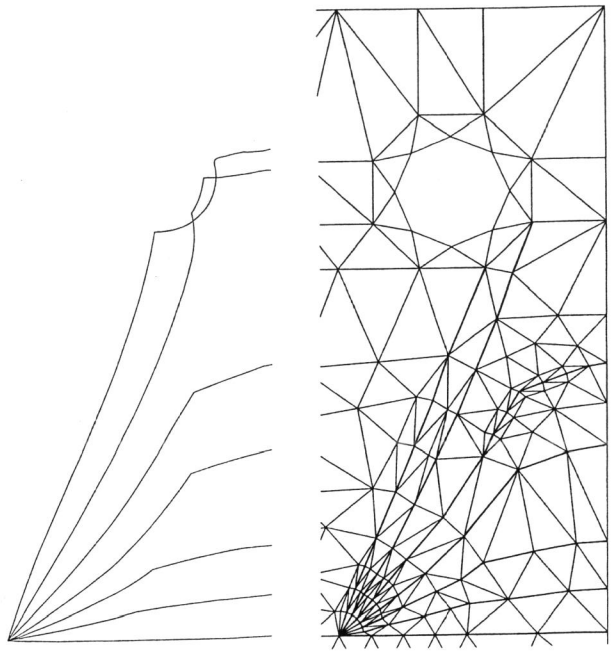

Fig. 8 Experimentally obtained and FE-modelled mixed-mode crack paths in CTS-specimens (α = 0-90 deg., $\Delta\alpha$ = 15 deg.)

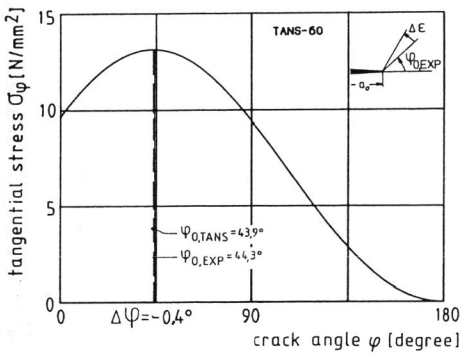

Fig. 9 Variation of tangential stress with $\Delta\varepsilon$ for crack lenght a_0, α = 60 deg.

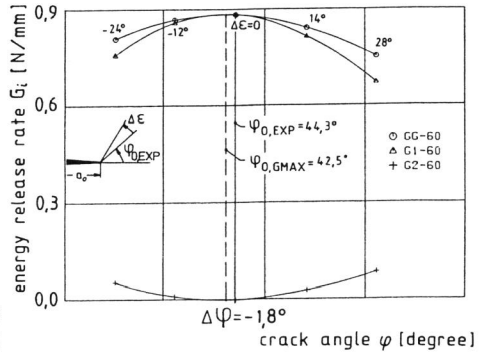

Fig. 10 Variation of energy release rates with $\Delta\varepsilon$ for crack lenght $a_0 + \Delta\bar{a}$, α = 60 deg.

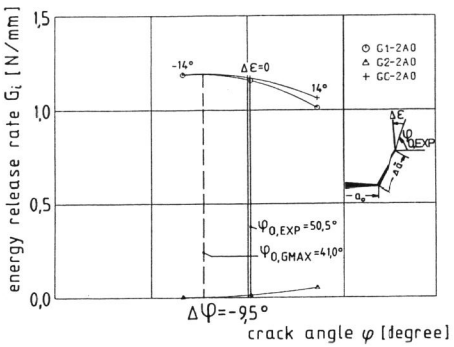

Fig. 11 Variation of energy release rates with $\Delta\varepsilon$ for crack lenght $a_0 + 2\Delta\bar{a}$, α = 60 deg.

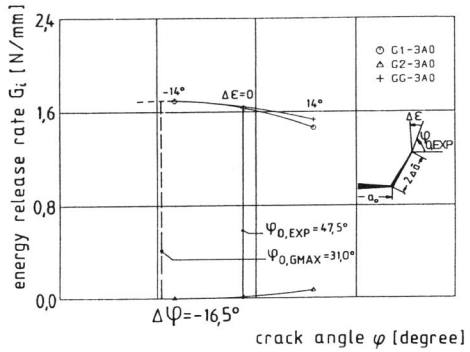

Fig. 12 Variation of energy release rates with $\Delta\varepsilon$ for crack lenght $a_0 + 3\Delta\bar{a}$, α = 60 deg.

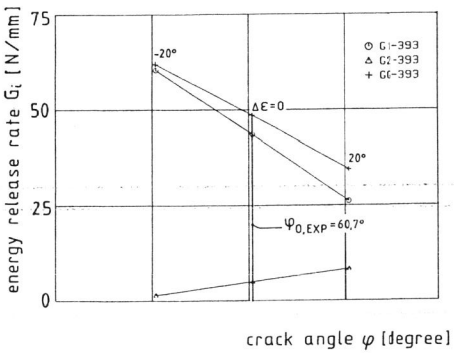

Fig. 13 Variation of energy release rates with $\Delta\varepsilon$ for crack lenght $a_0 + (n-1)\Delta\bar{a}$, α = 60 deg.

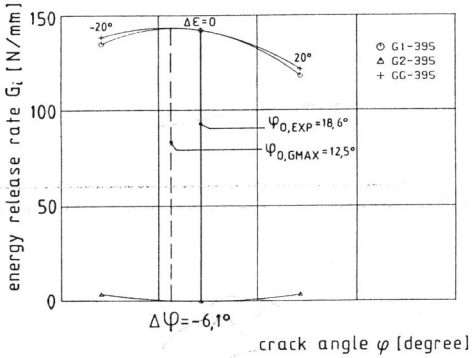

Fig. 14 Variation of energy release rates with $\Delta\varepsilon$ for crack lenght $a_0 + n\Delta\bar{a}$, α = 60 deg.